Send Orders for Reprints to reprints@benthamscience.ae

Current Pharmaceutical Analysis, 2016, *12*, 249-257

Fragmentation Study of *Daphniphyllum* Alkaloids by Electrospray Ionization Quadrupole Time-of-flight Mass Spectrometry

Min-Min Cao[a,c,d,#], Dan Wang[e,f,#], Hao Zhang[a], Dong-Mei Fang[b], Hong-Ping He[*a,c], Xiao-Jiang Hao[c], Guo-Lin Zhang[b] and Zhi-Jun Wu[*,b]

[a]*School of Pharmacy, Yunnan University of TCM, Kunming, P.R. China;* [b]*Chengdu Institute of Biology, Chinese Academy of Sciences, Chengdu, P.R. China;* [c]*State Key Laboratory of Phytochemistry and Plant Resources in West China, Kunming Institute of Botany, Chinese Academy of Sciences, Kunming, P.R. China;* [d]*University of Chinese Academy of Sciences Beijing, P.R. China;* [e]*Chengdu University, Chengdu, P.R.China;* [f]*West China School of Pharmacy Sichuan University, Chengdu, P.R. China*

Zhi-Jun Wu

Abstract: A series of 16 *Daphniphyllum* alkaloids isolated from *Daphniphyllum macropodum* were investigated by electrospray ionization quadrupole time-of-flight tandem mass spectrometry (ESI-QTOF-MS/MS) in positive-ion mode. Deuterium labeling experiments were carried out to identify the major product ions. Although compounds have similar structures, the profiles of their MS/MS spectra vary greatly. For compounds **1** and **2**, abundant product ions both in high and low mass range can be detected. A six-member H rearrangement and the cleavage of C1-C2 bond connecting rings A, C and D play an important role in providing the product ions in low mass range. For compounds **3**-**9**, the relative abundance of product ions in low mass range is low. This may result from the loss of HCOOCH3 occurring readily because C4-C5 double bond prevents six-member H rearrangement. Main fragmentation patterns of compounds **10**-**14** are the loss of the different side-chain groups and the cleavage of pyrrol and pyridine rings. A series of ion clusters detected in low mass range are characteristic ions for compounds **10**-**14**. Fragmentation patterns of compounds **15** and **16** were elucidated. Four groups of isomers in these compounds were distinguished by characteristic product ions or fragmentation patterns.

Keywords: *Daphniphyllum* alkaloids, electrospray, ESI-QTOF, six-member H rearrangement, fragmentation, isomers.

1. INTRODUCTION

Daphniphyllum alkaloids are a family of natural products with complex polycyclic systems [1-2]. In recent years, many new *Daphniphyllum* alkaloids with novel skeletons have been isolated and identified [2-14], and some of them exhibit biological properties such as cytotoxicity against murine lymphoma L1210 cells [3-5], cytotoxicity against two tumor cell lines, P-388 and A-549 [6], cytotoxicity against human cancer cell lines [7], antioxidant activity [8], moderate vasorelaxant effects on the rat aorta [9]. *Daphniphyllum* alkaloids with unique structural features have attracted great interest for total synthesis [15] and biosynthetic research [16].

Mass spectrometry (MS), coupled with electrospray ionization (ESI), has been an important physicochemical methods for the identification of trace natural products [17-21]. ESI-MS is rapid and sensitive, and can be coupled to separation techniques such as high performance liquid chromatography (HPLC) and capillary electrophoresis (CE). As a result, the technique is used extensively in analyzing drugs, natural products, pesticides, and other small molecules. Obtaining sufficient characteristic structural information of known natural products can contribute to identifying their degradation products, metabolites, and biosynthetic intermediates. Herein, the detailed fragmentation of a series of *Daphniphyllum* alkaloids were studied with collision-induced dissociation (CID)-MS/MS using an electrospray ionization (ESI) quadrupole time-of-flight (QTOF) MS/MS hybrid instrument in positive-ion mode.

2. EXPERIMENTAL

2.1. Chemicals and Samples

HPLC-grade methonol was obtained from Fisher Scientific (Pittsburgh, PA, USA), CD_3OD from Cambridge Isotope Laboratories (Andover, MA, USA) and mass calibration standards from Agilent Technologies (Santa Clara, CA, USA). The isolation and structural determinations of the series of Daphniphyllum alkaloids (Daphmacromine A, Daphmacromine C, Daphmacromine E, Daphmacromine G, Daphmacromine H, Daphmacromine M, Daphmacromine O, Daphnezomine K, Daphnezomine T, Daphhimalenine B, Daphnezomines U, Daphtenidine C, Daphtenidine D, Deoxyyuzurimine, macropodumine G, Yuzurimine, Yuzurimine

*Address correspondence to these authors at the Chengdu Institute of Biology, Chinese Academy of Sciences, Chengdu, China, Box: 610041, Chengdu, P.R. China; Tel: +86-28-82890717; Fax: +86-28-82890288; E-mails: *wuzj@cib.ac.cn*; hehongping@mail.kib.ac.cn

[#]These authors contributed equally to this work.

1875-676X/16 $58.00+.00

C; Fig. **1**) have been described in detail previously [5, 7, 10-11].

2.2. Mass Spectrometry

High-resolution experiments were performed on a Bruker micrOTOF-Q mass spectrometer (Bremen, Germany) with an ESI source in the positive-ion mode. The capillary voltage was maintained at –4500 V with the end plate offset at –500 V. Nitrogen was used as the drying and nebulizing gas at a flow rate of 4.0 L/min and a pressure of 0.3 bar, respectively. The drying gas temperature was maintained at 180 °C. Argon was introduced into the collisional cell as the collision gas. The introduction rate of samples was 180 µl/h. The samples were dissolved in methanol (concentration: 1 pmol/µl) and the diluent was directly injected into the mass spectrometer. The collision energy was optimized to achieve sufficient fragmentation. MS/MS/MS spectra were obtained when the in-source CID was set at 80 eV. The mass data were processed with Bruker Compass DataAnalysis 4.0.

3. RESULTS AND DISCUSSION

A total of 16 *Daphniphyllum* alkaloids were investigated by CID-MS/MS in positive-ion mode. For all the compounds, the precursor $[M+H]^+$ ions were selected and the product ions were recorded by ESI-QTOF-MS/MS.

3.1. Structural Analysis of Compounds

3.1.1. CID MS of Compounds 1–2

The precursor $[M+H]^+$ ion at *m/z* 486 for daphtenidine D (**1**) was analyzed using CID-MS/MS and corresponding MS/MS spectrum was shown in Fig. (**2**). The exact masses of major product ions are provided in Table **1**. The loss of

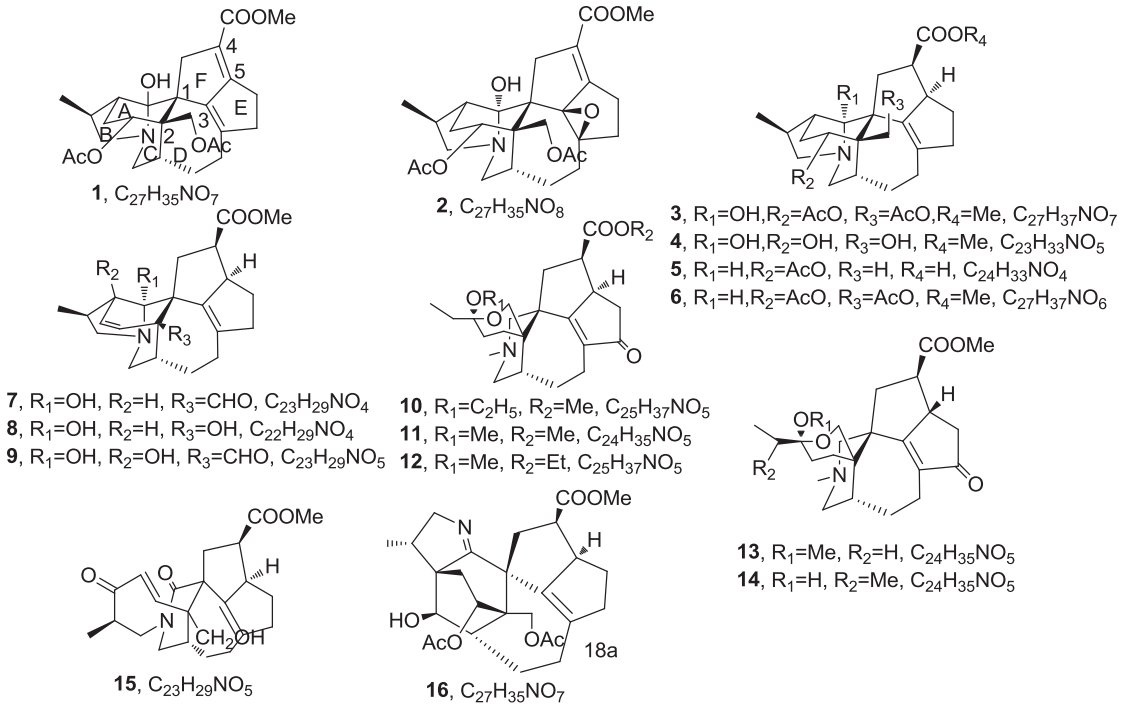

Fig. (1). *Daphniphyllum* alkaloids: Daphtenidine D (**1**, ***Mr*** 485.2414); Daphmacromine O (**2**, ***Mr*** 501.2362); Yuzurimine (**3**, ***Mr*** 487.2570); Daphnezomine K (**4**, ***Mr*** 403.2359); Daphmacromine M (**5**, ***Mr*** 399.2410); Deoxyyuzurimine (**6**, ***Mr*** 471.2621); Daphhimalenine B (**7**, ***Mr*** 383.2097); Daphnezomine T (**8**, ***Mr*** 371.2097); Yuzurimine C (**9**, ***Mr*** 399.2046); Daphmacromine C (**10**, ***Mr*** 431.2672); Daphmacromine E (**11**, ***Mr*** 417.2515); Daphmacromine A (**12**, ***Mr*** 431.2672); Daphmacromine G (**13**, ***Mr*** 417.2515); Daphmacromine H (**14**, ***Mr*** 417.2515); Daphnezomine U (**15**, ***Mr*** 399.2046); Daphtenidine C (**16**, ***Mr*** 485.2414).

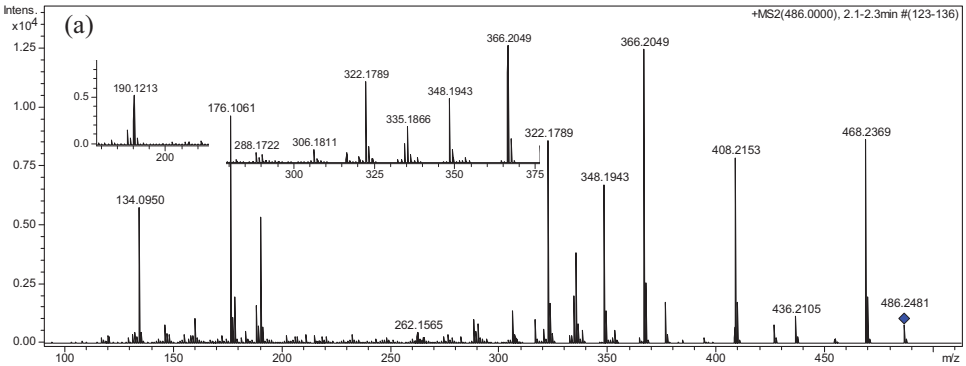

Fig. (2). Contd…

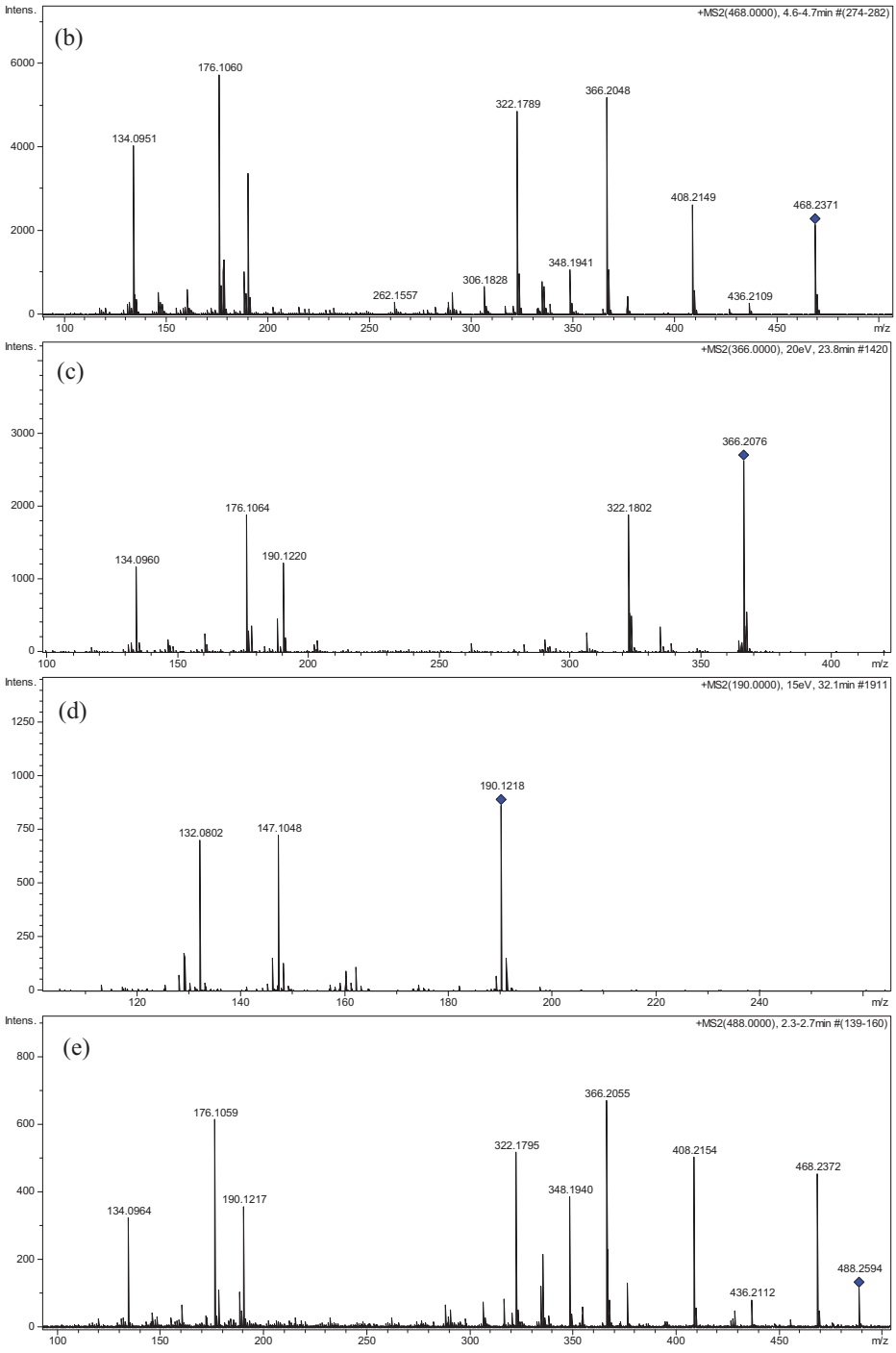

Fig. (2). MS/MS and MS/MS/MS spectra of daphtenidine D (**1**): (**a**) selected $[M + H]^+$ at *m/z* 486(collision energy at 35 eV; insertion is the amplified spectrum), (**b**) selected ion at *m/z* 468 from *m/z* 486 (collision energy at 30 eV), (**c**) selected ion at *m/z* 366 from *m/z* 486 (collision energy at 20 eV), (**d**) selected ion at *m/z* 190 from *m/z* 366 (collision energy at 15 eV), and deuterated daphtenidine D (**1**) (collision energy at 35 eV).

the different side-chain groups and the cleavage of rings A, C and D are main fragmentation patterns (Scheme **1**).

The product ions at *m/z* 468, 436, 426, 408, and 376 were formed from the precursor ion at *m/z* 486 by losses of H_2O, CH_2CO, MeOH or AcOH, or their simultaneous losses. Interestingly, a radical product ion at *m/z* 335 resulting from the homolytic cleavage of C2-C3 bond (Fig. **1**) was detected. The product ion at *m/z* 366 was formed by loss of an AcOH molecule from *m/z* 426. The processes involve six-member H rearrangement and the cleavage of C1-C2 bond connecting rings A, C and D. High tension of C1-C2 bond connecting three rings and low activation energy of six-member transition state may drive the fragmentation reaction. In addition, the new double bond generated from six-member H rearrangement can form conjugation system with original C4-C5 double bond, which facilitates the processes [21]. The product ion at *m/z*

Table 1. Elemental constituents of major product ions from $[M+H]^+$ for daphtenidine D (1) (collision energy: 35 eV).

Ion	Formula	Calculated	Observed	Error(ppm)
$[M+H]^+$	$C_{27}H_{36}O_7N$	486.2486	486.2481	1.0
$[M+H-H_2O]^+$	$C_{27}H_{34}O_6N$	468.2381	468.2369	2.4
$[M+H-H_2O-CH_3OH]^+$	$C_{26}H_{30}O_5N$	436.2118	436.2105	3.0
$[M+H-H_2O-CH_2CO]^+$	$C_{26}H_{30}O_5N$	426.2275	426.2254	4.8
$[M+H-H_2O-CH_2CO-H_2O]^+$	$C_{25}H_{30}O_4N$	408.2169	408.2153	3.9
$[M+H-H_2O-CH_3OH-AcOH]^+$	$C_{24}H_{26}O_3N$	376.1907	376.1904	1.0
$[M+H-H_2O-CH_2CO-AcOH]^+$	$C_{23}H_{28}O_3N$	366.2064	366.2049	3.9
$[M+H-H_2O-CH_2CO-H_2O-AcOH]^+$	$C_{23}H_{26}O_2N$	348.1958	348.1943	4.3
$[M+H-H_2O-CH_2CO-H_2O-CH_2OAc]^+$	$C_{22}H_{25}O_2N$	335.1880	335.1866	4.1
$[M+H-H_2O-CH_2CO-H_2O-CH_3OAc]^+$	$C_{22}H_{25}O_2N$	334.1802	334.1790	3.6
$[M+H-H_2O-CH_2CO-AcOH-C_2H_4O]^+$	$C_{21}H_{24}O_2N$	322.1802	322.1789	3.8
$[M+H-H_2O-CH_2CO-AcOH-C_{11}H_{12}O_2]^+$	$C_{12}H_{16}ON$	190.1226	190.1213	7.0
$[M+H-H_2O-CH_2CO-AcOH-C_{12}H_{14}O_2]^+$	$C_{11}H_{14}ON$	176.1070	176.1061	5.1
$[C_9H_{12}N]^+$	$C_9H_{12}N$	134.0964	134.0950	10.2

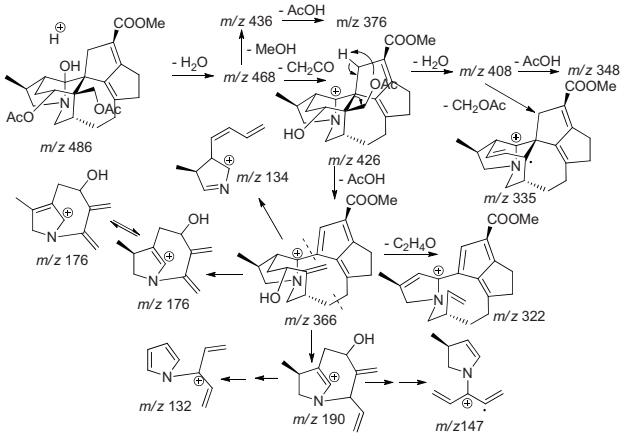

Scheme 1. Major fragmentation patterns of $[M+H]^+$ for daphtenidine D (1).

322 was formed by loss of C_2H_4O from product ion at *m/z* 366. The product ions at *m/z* 190, 176 and 134 in low mass range are characteristic ions, which resulted from *m/z* 366 by the cleavage of rings A, C and D. The product ions at m/z 147 and 132 resulting from the product ion at *m/z* 190 by loss of C_2H_3O and C_3H_6O respectively (Fig. **2d**), further supported its structure. A labeling experiment involving H/D exchange of compound **1** was carried out and corresponding MS/MS spectrum was consistent with the proposed fragmentation pathways (Fig. **2e**). Main fragmentation patterns of daphmacromine O (**2**) are similar to that of daphtenidine D (**1**).

3.1.2. CID MS of Compounds 3–6

The C4-C5 double bond in compound (**1**) substituted by single bond affords yuzurimine (**3**). Although their structures are very similar, the profile of corresponding MS/MS spectra varies greatly (Figs. (**2a** and **3a**)). The neutral losses of AcOH, CH_2CO, H_2O and HCOOMe are major fragmentation patterns for compound **3**. Main product ions were formed from the precursor ion at *m/z* 488 by single loss or their combinations (supporting information). The reason of fragmentation difference between compounds **1** and **3** might be that the loss of HCOOMe occurs readily and the new generation of double bond prevents six-member H rearrangement. This leads to the cleavage of C1-C2 bond becomes difficult. Thus, the product ions in low mass range formed by the cleavage of rings A, B and C, are very weak. For daphnezomine K (**4**), the neutral losses of H_2O, MeOH and HCOOMe are major fragmentation patterns. Low-abundance product ions at *m/z* 190, 176 and 134 were detected. For daphmacromine M (**5**), the product ion at *m/z* 340 formed by loss of AcOH from the precursor $[M+H]^+$ ion at *m/z* 400. The product ions in low mass range might be formed by the cleavage of rings A, B and C, accompanied with the loss of N-atom (supporting information). Although loss of HCOOH is difficult to occur, no O-atom linked to C3 prevents six-member H rearrangement. Thus, the product ions

at *m/z* 190, 176 and 134 were not detected. This supports the proposed fragmentation mechanisms. The fragmentation patterns of deoxyyuzurimine (**6**) in high mass range are similar to that of compound **3**, but in low mass range similar to that of compound **5**. The fragmentation difference in low mass range between compounds **3**, **4** and **5**, **6** might be the different protonation sites. For compounds **5** and **6**, the protonation site is located at N-atom, which leads to the neutral losses including N-atom.

3.1.3. CID MS of Compounds 7–9

Ring A is cyclohexene in daphhimalenine B (**7**), daphnezomine T (**8**), and yuzurimine C (**9**). The neutral losses of H_2O, CO, HCOOMe are main fragmentation patterns from daphhimalenine B (**7**) (Fig. **3b**). The loss of CO indicates the formyl group. For compounds 7-**9**, the neutral loss of 60 Da corresponds to HCOOMe. There are no product ions similar to that of compounds **1** and **2** in low mass range, which supported proposed processes of six-member H rearrangement.

3.1.4. CID MS of Compounds 10–14

The structures of daphmacromine C (**10**), daphmacromine E (**11**), and daphmacromine A (**12**) are very similar. Compound **10** was selected as a representative compound for the following analysis. Main product ions (Table **2**) in high mass range were formed by the loss of the different side-

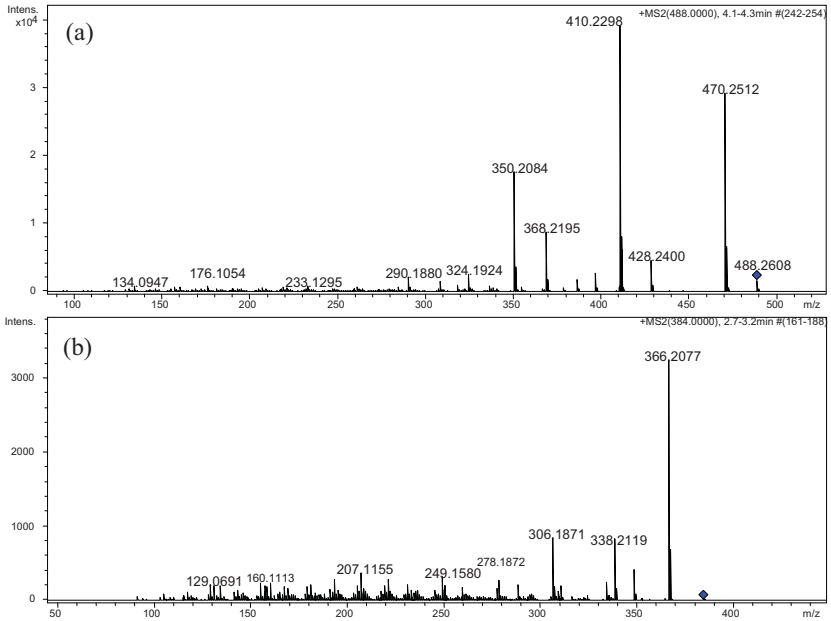

Fig. (3). Product ion scan of the selected precursor $[M+H]^+$ (**a**) at *m/z* 488 for yuzurimine (**3**) (collision energy: 35 eV), (**b**) at *m/z* 384 for Daphhimalenine B (**7**) (collision energy: 35 eV).

Table 2. Elemental constituents of major product ions from $[M+H]^+$ for daphmacromine C (10) (collision energy: 35 eV).

Ion	Formula	Calculated	Observed	Error(ppm)
$[M+H]^+$	$C_{25}H_{38}O_5N$	432.2744	432.2735	2.1
$[M+H-CH_2O]^+$	$C_{24}H_{36}O_4N$	402.2651	402.2662	-3.1
$[M+H-C_2H_5OH]^+$	$C_{23}H_{32}O_4N$	386.2326	386.2338	-3.2
$[M+H-CH_2O-C_2H_6]^+$	$C_{22}H_{30}O_4N$	372.2169	372.2176	-1.8
$[M+H-CH_2O-C_2H_5OH]^+$	$C_{22}H_{30}O_3N$	356.2220	356.2210	2.8
$[M+H-CH_2O-C_2H_5OH-CH_3NH_2]^+$	$C_{21}H_{25}O_3$	325.1798	325.1810	-3.7
$[M+H-CH_2O-C_2H_5OH-CH_3NCH_2]^+$	$C_{20}H_{25}O_3$	313.1798	313.1794	1.5
$[M+H-C_2H_5OH-C_5H_8O]^+$	$C_{18}H_{24}O_3N$	302.1751	302.1759	-2.8
$[M+H-CH_2O-C_2H_5OH-COOMe]^{+\cdot}$	$C_{20}H_{17}ON$	287.1305	287.1315	-3.6
$[M+H-CH_2O-C_2H_5OH-CH_3NCH_2-HCOOMe]^+$	$C_{18}H_{21}O$	253.1587	253.1572	5.8
$[M+H-C_2H_5OH-C_5H_8O-CH_3NCH_2-HCOOMe]^+$	$C_{14}H_{15}O$	199.1117	199.1125	-3.8
$[M+H-C_2H_5OH-C_5H_8O-CH_3NCH_2-HCOOMe-H_2O]^+$	$C_{14}H_{13}$	181.1012	181.1013	-0.8
$[C_7H_{13}O]^+$	$C_7H_{13}O$	113.0961	113.0957	3.5

chain groups or the cleavage of pyrrol and pyridine rings from the precursor ion at *m/z* 432 (Fig. **4** and Scheme **2**). The product ion at *m/z* 386 was formed by loss of C_2H_5OH from *m/z* 432, and affords the product ion at *m/z* 302 by the cleavage of pyrrol ring. The product ion at *m/z* 199 was formed from *m/z* 302 by sequential loss of CH_3NCH_2 and $HCOOCH_3$. The loss of CH_3NCH_2 involves four-member H rearrangement [22]. The product ion at *m/z* 356 was formed by loss of C_2H_5OH from the product ion at *m/z* 402, resulting from *m/z* 432 by the loss of CH_2O.

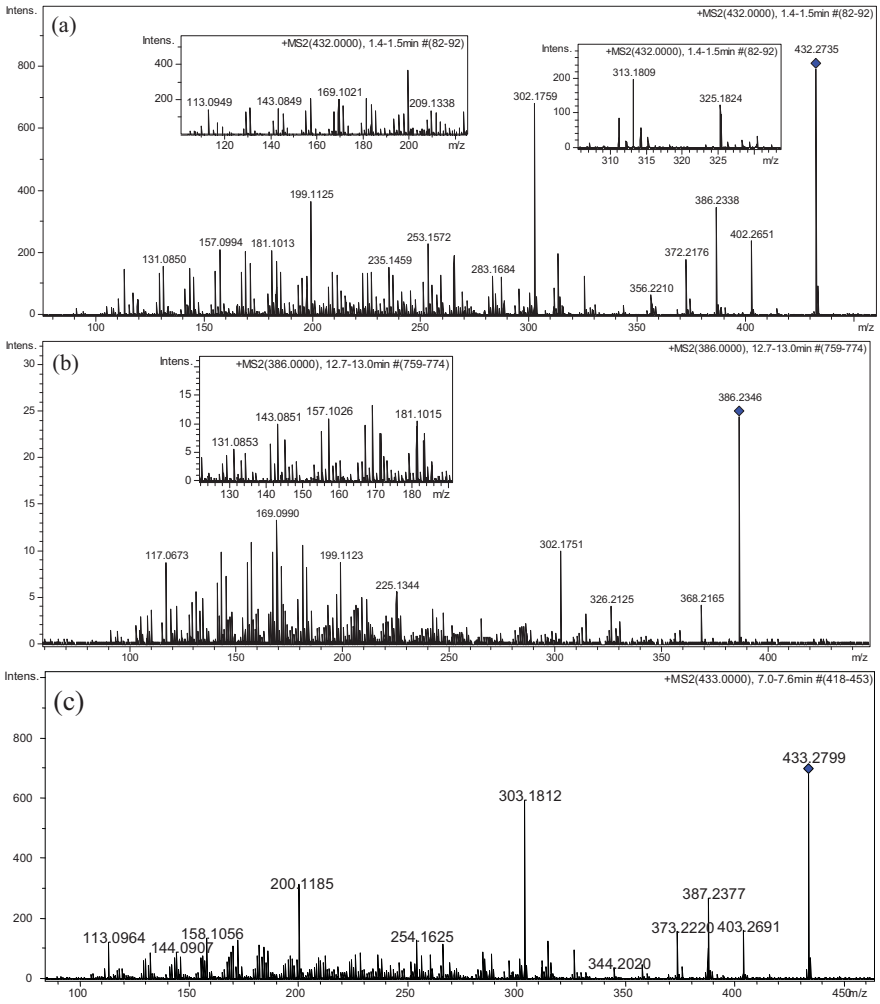

Fig. (4). MS/MS and MS/MS/MS spectra of daphmacromine C (**10**): (**a**) selected $[M + H]^+$ at *m/z* 432 (collision energy at 35 eV, insertion is the amplified spectrum), (**b**) selected ion at *m/z* 386 from *m/z* 432 (collision energy at 30 eV, insertion is the amplified spectrum), and deuterated daphmacromine C (**10**) (collision energy at 35 eV).

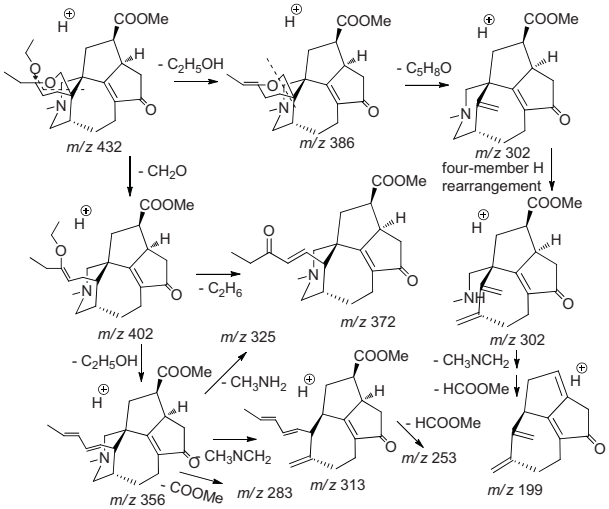

Scheme 2. Major fragmentation patterns of $[M+H]^+$ for daphmacromine C (10).

The product ion at *m/z* 356 was formed by loss of C_2H_5OH from the product ion at *m/z* 402, resulting from *m/z* 432 by the loss of CH_2O. The product ions at *m/z* 325, 313, and 283 were formed from *m/z* 356 by losses of CH_3NH_2, CH_3NCH_2, and $COOCH_3$, respectively. The neutral losses including N-atom occur readily, which implies that the protonation site is located at N-atom. D-labelled experiment (Fig. **4c**) supported the proposed fragmentation patterns. In low mass range, a series of ion clusters was detected. The difference of each cluster is 14 Da. H transfer leads to several peaks in each cluster. Main fragmentation patterns and profiles of MS/MS spectra of compounds **11** and **12** are similar to that of compound **10**. Daphmacromine G (**13**) and daphmacromine E (**11**) are a pair of diastereoisomers and their fragmentation patterns are similar. However, the relative abundance of product ions at *m/z* 386 and 302 vary greatly (Fig. **6**). For daphmacromine H (**14**), the neutral losses of H_2O, and CH_2O are main fragmentation patterns in high mass range.

3.1.5. CID MS of Compounds 15–16

The MS/MS spectra of daphnezomines U (**15**) were shown in Fig. (**5**) and main fragmentation pathways were shown in Scheme **3**. The exact masses of major product ions

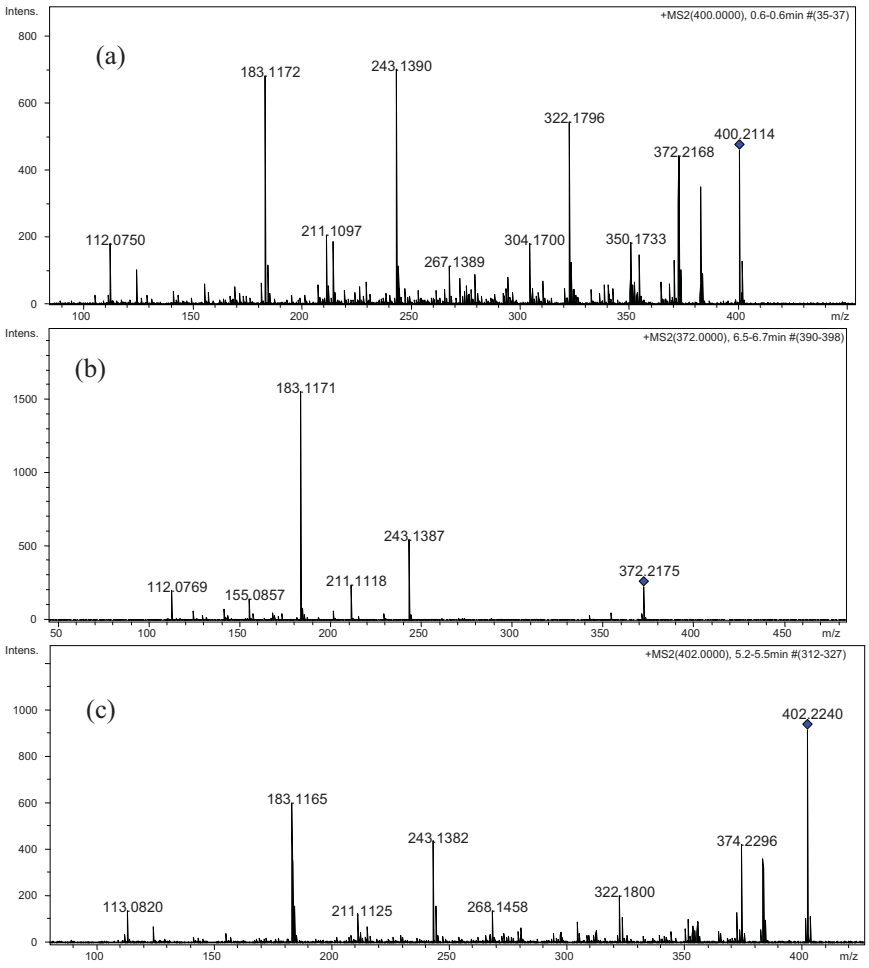

Fig. (5). MS/MS and MS/MS/MS spectra of daphnezomines U (**15**): (**a**) selected $[M + H]^+$ at *m/z* 400 (collision energy at 20 eV), (**b**) selected ion at *m/z* 372 from *m/z* 400 (collision energy at 25 eV), and (**c**) deuterated daphnezomines U (**15**) (collision energy at 20 eV).

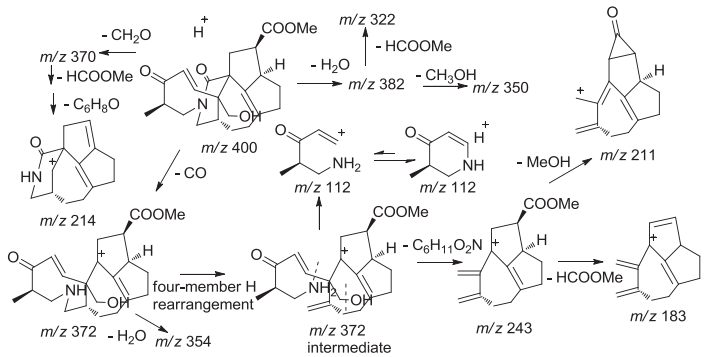

Scheme 3. Major fragmentation patterns of $[M+H]^+$ for daphnezomines U (15).

Table 3. Elemental constituents of major product ions from $[M+H]^+$ for daphtenidine D (15) (collision energy: 35 eV).

Ion	Formula	Calculated	Observed	Error (ppm)
$[M+H]^+$	$C_{23}H_{30}O_5N$	400.2118	400.2114	1.2
$[M+H-H_2O]^+$	$C_{23}H_{28}O_4N$	382.2013	382.3013	-0.2
$[M+H-CO]^+$	$C_{22}H_{30}O_4N$	372.2169	372.2168	0.3
$[M+H-CH_2O]^+$	$C_{22}H_{28}O_4N$	370.2013	370.2003	2.6
$[M+H-CO-H_2O]^+$	$C_{22}H_{28}O_3N$	354.2064	354.2042	6.2
$[M+H-H_2O-CH_3OH]^+$	$C_{22}H_{24}O_3N$	350.1751	350.1733	5.2
$[M+H-H_2O-HCOOMe]^+$	$C_{21}H_{24}O_2N$	322.1802	322.1796	1.6
$[M+H-CO-C_6H_{11}O_2N]^+$	$C_{16}H_{19}O_2$	243.1380	243.1390	-4.4
$[M+H-CH_2O-HCOOMe-C_6H_8O]^+$	$C_{14}H_{16}ON$	214.1226	214.1222	1.9
$[M+H-CO-C_6H_{11}O_2N-MeOH]^+$	$C_{15}H_{15}O$	211.1117	211.1097	9.5
$[C_6H_{10}ON]^+$	$C_6H_{10}ON$	112.0757	112.0750	6.1

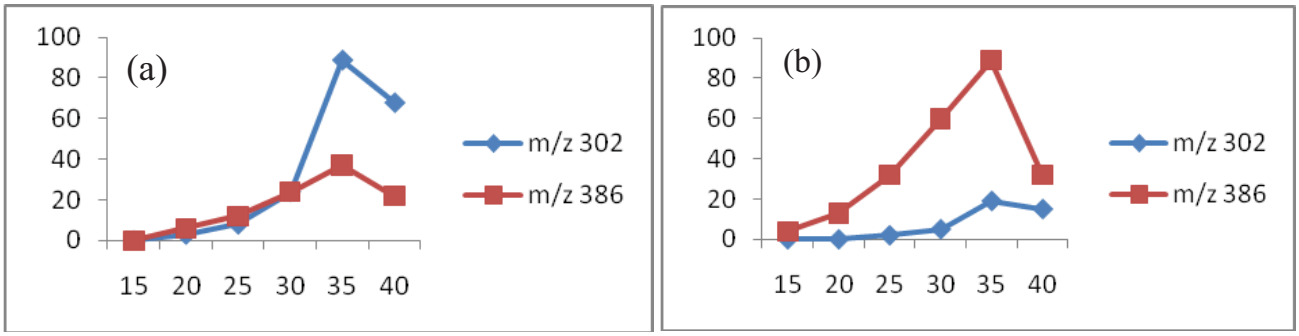

Fig. (6). The relative abundance of ions at *m/z* 386 and 302 in MS/MS spectra of $[M+H]^+$ expressed as a function of collision energy: (**a**) daphmacromine E (**11**) and (**b**) daphmacromine G (**13**).

are provided in Table **3**. The neutral losses of H_2O, CO, CH_2O, CH_3OH, HCOOMe and cleavage of nine-member ring including α, β-unsaturated carbonyl are main fragmentation patterns. The product ion at *m/z* 372 was formed by loss of CO from the precursor ion at *m/z* 400 and further produces a pair of ions at *m/z* 243 and 112 (Fig. **5b**). The processes go through an intermediate formed by four-member H rearrangement. The product ion at *m/z* 243 affords the product ions at *m/z* 211 and 183 by losses of CH_3OH and HCOOMe, respectively. The proposed fragmentation patterns are in accordance to the D-labelled spectrum (Fig. **5c**). For daphtenidine C (**16**), main fragmentation patterns are the losses of AcOH, HCOOMe, CH_2CO, and H_2O.

3.2. Distinction of Isomers

Distinction of isomers is interesting [22]. There are four groups of isomers in these compounds, compounds **1** and **16**, compounds **5**, **9** and **15**, compounds **10** and **12**, and compounds **11**, **13** and **14**. For compounds **1**, the loss of H_2O and cleavage of rings A, C and D occur readily. However, the product ions resulting from loss of H_2O and cleavage of rings show low relative abundance for compound **16**. For compounds **10** and **12**, the product ions at *m/z* 302 and 316 formed by cleavage of pyrrol ring from precursor ions respectively can be used to distinguish the two isomers. The profiles of MS/MS spectra of compounds **5**, **9** and **15** vary greatly. The loss of AcOH and sequential losses of H_2O are characteristic fragmentation patterns for compounds **5** and **9** respectively. High- abundance product ions formed by cleavage of skeleton in low mass range can be detected for compound **15**. Although compounds **11** and **13** are diastereoisomers, relative abundance of the product ions at *m/z* 386 and 302 vary (Fig. **6**) and can be used to distinguish the two compounds. The characteristic product ion at *m/z* 400 in MS/MS spectrum of compound **14** indicates the present of hydroxyl, which is different from compounds **11** and **13**.

CONCLUSION

The CID fragmentation pathways of a total of 16 *Daphniphyllum* alkaloids were elucidated using ESI-QTOF-MS/MS in positive-ion mode. Although the structures of compounds **1**-**9** are similar, the profiles of MS/MS spectra vary greatly. A six-member H rearrangement plays an important role in providing the product ions in low mass range. For compounds **10**-**14**, the loss of the different side-chain groups and the cleavage of pyrrol and pyridine rings are main frag-

mentation patterns. The proton was located at N-atom, which leads to a series of ion clusters in low mass range for these compounds. Four groups of isomers were distinguished by characteristic product ions or fragmentation patterns. In addition, a radical ion was detected. In summary, abundant information obtained from fragmentation experiments of $[M+H]^+$ precursor ions is especially valuable for rapid identification of these *Daphniphyllum* alkaloids.

CONFLICT OF INTEREST

The authors confirm that this article content has no conflict of interest.

ACKNOWLEDGEMENTS

This work was supported by the National Natural Science Foundation of China (Nos. 21305137), CAS Key Technology Talent Program and the Infrastructure Projectsfor Application of Department of Science in Sichuan Province.

SUPPLEMENTARY MATERIAL

Supplementary material is available on the publisher's web site along with the published article.

REFERENCES

[1] Yamamura, S.; Irikawa, H.; Okumura, Y.; Hirata, Y. The structure of yuzurimine-C. *Bull. Chem. Soc. Jpn.* **1975**, *48*, 2120-2123.

[2] Kobayashi, J.; Kubota, T. The *Daphniphyllum* alkaloids. *Nat. Prod. Rep.* **2009**, *26*, 936-962.

[3] Morita, H.; Yoshida, N.; Kobayashi. J. Daphnezomines H, I, J, and K, new daphnilactone-type and yuzurimine-type alkaloids from *Daphniphyllum humile*. *Tetrahedron.* **2000**, *56*, 2641-2646.

[4] Kubota, T.; Matsuno, Y.; Morita, H.; Shinzato, T.; Sekiguchid, M.; Kobayashi, J. Daphtenidines A–D, new *Daphniphyllum* alkaloids from *Daphniphyllum teijsmannii*. *Tetrahedron*. **2006**, *62*, 4743-4748.

[5] Zhang, Y.; He, H. P.; Di, Y. T.; Mu, S. Z.; Wang, Y. H.; Wang, J. S.; Li, C. S.; Kong, N. C.; Gao, S.; Hao .X. J. Paxiphyllines A and B, new alkaloids from *Daphniphyllum paxianum*. *Tetrahedron Lett.* **2007**, *48*, 9104-9107.

[6] Toda, M.; Hirata, Y.; Yamamura. S. Daphniphyllum alkaloids—II: Secodaphniphylline and methyl homosecodaphniphyllate. *Tetrahedron*, **1972**, *28*, 1477-1484.

[7] Cao, M. M.; Zhang,; He, Y.H. P.; Li, S. F.; Huang, S. D.; Chen, D. Z.; Tang, G. H.; Li, S. L.; Di, Y. T.; Hao, X. J. Daphmacromines A−J, alkaloids from *Daphniphyllum macropodum*. The isolation and structures of daphniteijsmine, daphnijsmine and desacetyldaphnijsmine. *J. Nat. Prod.* **2012**, *75*, 1076-1082.

[8] Yamamura, S.; Hirata, Y. Pordamacrines A and B, alkaloids from *Daphniphyllum macropodum*. *Tetrahedron Lett.,* **1974**, *15*, 2849.

[9] Matsuno, Y.; Okamoto, M.; Hirasawa, Y.; Kawahara, N.; Goda, Y.; Shiro, M.; Morita, H. Morita. Pordamacrines A and B, alkaloids from *Daphniphyllum macropodum*. *J. Nat. Prod.* **2007**, *70*, 1516-1518.

[10] Zhang, Y.; Di, Y. T.; Zhang, Q.; Mu, S. Z.; Tan, C. J.; Fang, X.; He, H. P.; Li, S. L.;Hao, X. *J.* Daphhimalenine A, a new alkaloid with an unprecedented skeleton, from *Daphniphyllum himalense*. *Org. Lett*. **2009**, *11*, 5414-5417.

[11] Cao, M. M.; Wang, L.; Zhang, Y.; He, H. P.; Gu, Y. C.; Zhang, Q.; Li, Y. C.; Yuan, M.; Li, S. L.; Di, Y. T.; Hao, X. Daphmacromines K–O, alkaloids from *Daphniphyllum* macropodum. *Fitoterapia.* **2013**, 89, 205-209.

[12] Li, Z. Y.; Chen, P.; Xu, H. G.; Peng, S. Y.; Yang, Y.; Zhao, Z. Z.; Guo, Y. W. Further *Daphniphyllum* alkaloids from the leaves of Daphniphyllum macropodum. *Miq. HeIv. Chim. Acta.* **2007***, 90,* 1353-1359.

[13] Kubota, T.; Suzuki, T.; Ishiuchi, K.; Kuhara, T.; Kobayashi. J. Daphnezomines T—V, alkaloids from *Daphniphyllum humile*. *Chem. Pharm. Bull.* **2009**, *57*, 504-507.

[14] Li, Z. Y.; Gu, Y. C.; Irwin, D.; Sheridan, J.; Clough, J.; Chen, P.; Peng, S. Y.; Yang, Y. M.; Guo. Y. W. Further *Daphniphyllum* alkaloids with insecticidal activity from the bark of *Daphniphyllum macropodum*Miq. *Chem. Biodivers.* **2009**, *6*, 1744-1750.

[15] Wallace, G. A.; Heathcock, C. H. Further studies of the *Daphniphyllum* alkaloid polycyclization cascade. *J. Org. Chem.* **2001**, *66*, 450-454.

[16] Niwa, H.; Hirata, Y.; Suzuki, K. T.; Yamamura, S. Biosynthesis of daphnilactone-B. *Tetrahedron Lett.* **1973**, *14*, 2129-2132.

[17] Yang, M.; Sun, J. H.; Lu, Z. Q.; Chen, G. T.; Guan, S. H.; Liu, X.; Jiang, B. H.; Ye, Min.; Guo, D. A. Phytochemical analysis of traditional Chinese medicine using liquid chromatography coupled with mass spectrometry. *J. Chromatogr. A*. **2009**, *1216*, 2045-2062.

[18] Wu, Z. J.; Wang, J.H.; Fang, D. M.; Zhang, G. L. Analysis of iridoid glucosides from paederia scandens using HPLC–ESI-MS/MS. *J. Chromatogr. B*. **2013**, *54*. 923-924,

[19] Guo, Z. Q.; Qi, H. Y.; Jiang, Y.; Fang, D. M.; Zhang, G. L.; Wu, Z. J. Analysis of a caffeic acid derivative by ESI–MS/MS: unexpected product ions formed by 'internal residue loss'. *J. Mass Spectrom.* **2014**, *49*, 428-431.

[20] Wu, Z. J.; Pu, J. X.; Li, L. M.; Fang, D. M.; Qi, H. Y.; Chen, J. Z.; Li, G. Y.; Sun, H. D.; Zhang, G. L. Electrospray tandemmass spectrometry of longipedlactone triterpenoids. *J. Mass Spectrom.* **2010**, *45*, 451-455.

[21] Wu, Z. J.; Sun, D. M.; Fang, D. M.; Chen, J. Z.; Cheng, P.; Zhang. G. L. Analysis of matrine-type alkaloids using ESI-QTOF. *Int. J. Mass spectrom.* **2013**, *28,* 341-342.

[22] Lu, C. C.; Wang, J. H.; Fang, D. M.; Wu, Z. J. Electrospray ionization tandem mass spectrometry of isomeric iridoid glucoside dimers**.** *Rapid Commun. Mass Sp.*, **2013**, *27,* 503-506.

Received: July 20, 2015 Revised: October 15, 2015 Accepted: October 22, 2015